

# Z-GMOT: Zero-shot Generic Multiple Object Tracking

Kim Hoang Tran<sup>1</sup>, Tien-Phat Nguyen<sup>2</sup>, Anh Duy Le Dinh<sup>2</sup>, Pha Nguyen<sup>3</sup>, Thinh Phan<sup>3</sup>,  
Khoa Luu<sup>3</sup>, Donald Adjeroh<sup>3</sup>, Ngan Hoang Le<sup>3</sup>

<sup>1</sup>FPT Software AI Center, Vietnam, <sup>2</sup>University of Arkansas, USA

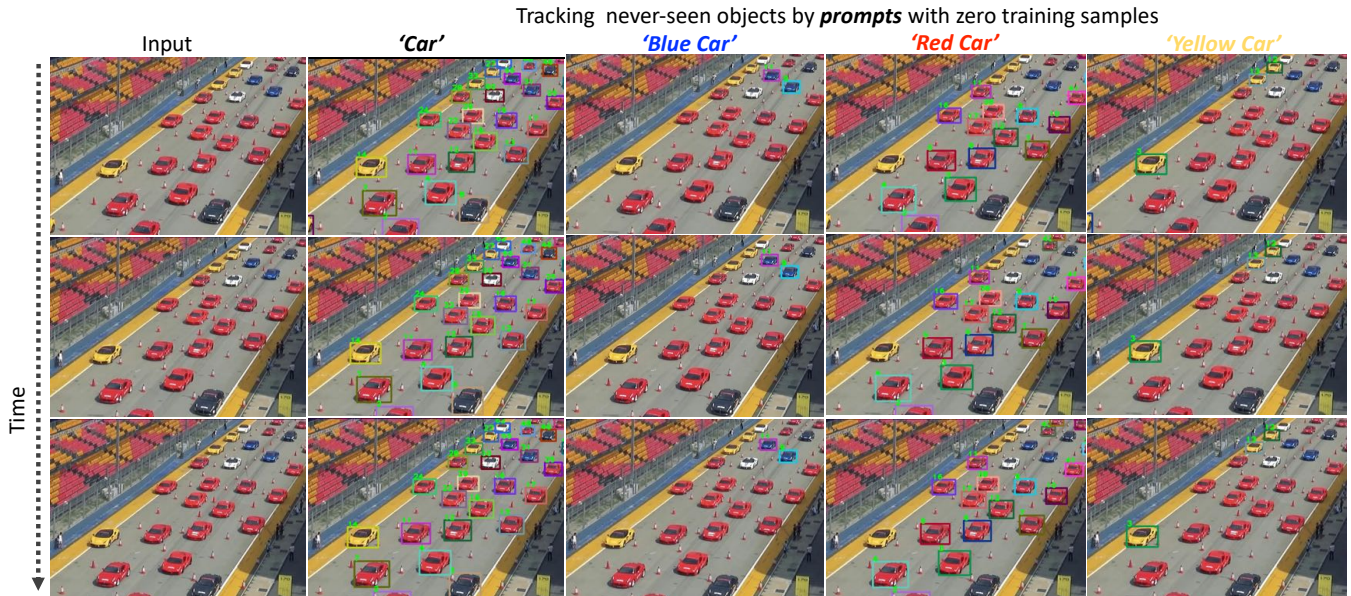


Figure 1: Z-GMOT tracks *unseen object categories with zero training examples*. Given a video (1<sup>st</sup> column), Z-GMOT can track a general object category ‘cars’ (2<sup>nd</sup> column) and specific objects category e.g., ‘blue cars’ (3<sup>th</sup> column), ‘red cars’ (4<sup>th</sup> column), ‘yellow cars’ (5<sup>th</sup> column).

## ABSTRACT

Despite the significant progress made in recent years, Multi-Object Tracking (MOT) approaches still suffer from several limitations, including their reliance on prior knowledge of tracking targets, which necessitates the costly annotation of large labeled datasets. As a result, existing MOT methods are *limited to a small set of predefined categories, and they struggle with unseen objects* in the real world. To address these issues, Generic Multiple Object Tracking (GMOT) has been proposed, which requires less prior information about the targets. However, all existing GMOT approaches follow a one-shot paradigm, *relying mainly on the initial bounding box and thus struggling to handle variants e.g., viewpoint, lighting, occlusion, scale, and etc.*

In this paper, we introduce a novel approach to address the limitations of existing MOT and GMOT methods. Specifically, we propose a **zero-shot GMOT (Z-GMOT)** algorithm that **can track**

**never-seen object categories with zero training examples**, without the need for predefined categories or an initial bounding box. To achieve this, we propose iGLIP, an improved version of Grounded language-image pretraining (GLIP), which can detect unseen objects while minimizing false positives. We evaluate our Z-GMOT thoroughly on the GMOT-40 dataset, AnimalTrack testset, DanceTrack testset. The results of these evaluations demonstrate a significant improvement over existing methods. For instance, on the GMOT-40 dataset, the Z-GMOT outperforms one-shot GMOT with OC-SORT by 27.79 points HOTA and 44.37 points MOTA. On the AnimalTrack dataset, it surpasses fully-supervised methods with DeepSORT by 12.55 points HOTA and 8.97 points MOTA. To facilitate further research, we will make our code and models publicly available upon acceptance of this paper.

## KEYWORDS

Multiple Object Tracking, MOT, Generic MOT, Unseen, Zero-Shot, Language-Driven, Prompt

## ACM Reference Format:

Kim Hoang Tran<sup>1</sup>, Tien-Phat Nguyen<sup>2</sup>, Anh Duy Le Dinh<sup>2</sup>, Pha Nguyen<sup>3</sup>, Thinh Phan<sup>3</sup>, Khoa Luu<sup>3</sup>, Donald Adjeroh<sup>3</sup>, Ngan Hoang Le<sup>3</sup>. 2018. Z-GMOT: Zero-shot Generic Multiple Object Tracking. In *Proceedings of ACM Conference (Conference’17)*. ACM, New York, NY, USA, 16 pages. <https://doi.org/XXXXXXX.XXXXXXX>

Permission to make digital or hard copies of all or part of this work for personal or classroom use is granted without fee provided that copies are not made or distributed for profit or commercial advantage and that copies bear this notice and the full citation on the first page. Copyrights for components of this work owned by others than ACM must be honored. Abstracting with credit is permitted. To copy otherwise, or republish, to post on servers or to redistribute to lists, requires prior specific permission and/or a fee. Request permissions from [permissions@acm.org](mailto:permissions@acm.org).

Conference’17, July 2017, Washington, DC, USA

© 2018 Association for Computing Machinery.

ACM ISBN 978-x-xxxx-xxxx-x/YY/MM...\$15.00

<https://doi.org/XXXXXXX.XXXXXXX>

## 1 INTRODUCTION

Multiple Object Tracking (MOT) aims to recognize, localize and track dynamic objects in a scene. It has become a cornerstone of dynamic scene analysis and is essential for many important real-world applications such as surveillance, security, autonomous driving, robotics, and biology. To accomplish this task, MOT Typically requires a list of semantic categories that need to be tracked in both training and testing sets. The availability of sufficient training data for each category [29, 37, 51] and recent advancements in object detection [8, 44, 60, 64], have led to significant progress in the field of MOT. Despite this progress, current MOT methods are limited to a specific number of object categories and usually focus on a specific category of interest, such as pedestrians [14, 29, 37] or objects in autonomous driving scenarios [5, 11], requiring prior knowledge of the tracking target.. Moreover, existing methods are still inadequate to support versatile open-world MOT due to three primary challenges. Firstly, large-scale training data for MOT is costly and labor-intensive to annotate. Secondly, the long-tail problem arises when finding sufficient training data for rare categories, presenting a significant challenge. Thirdly, MOT is limited by the pre-defined labels/categories, and it struggles with identifying and tracking unseen categories. These three issues make it difficult for MOT to handle open-world scenarios where object categories are not predetermined.

In contrast to MOT, which requires significant prior knowledge about the objects/categories to be tracked, Generic Multiple Object Tracking (GMOT) [33, 34] aims to address the aforementioned issues with less prior knowledge. GMOT is designed to track multiple objects of the same or similar generic type, making it applicable to various fields such as annotating, video editing, and animal behavior monitoring. Existing GMOT approaches [1, 33, 34] follow the one-shot paradigm, which uses the bounding box of a single target object in the first video frame to track all objects that belong to the same class. However, such an approach heavily relies on the initial bounding box and is limited in handling object variations, e.g., pose, illumination, occlusion, scale, texture, etc. For example, given a video as in Fig. 1, GMOT is unable to track all cars if the initial bounding box is around blue car.

In addition, the availability of image-text pairs on the Internet is abundant and cost-effective. Recently, there has been a surge of interest in Vision-Language (VL) models, which combine the ability to comprehend visual data with natural language processing capabilities. Several related tasks have been proposed and investigated, such as Visual Question Answering [35, 48], Visual Reasoning [23, 49], Image Captioning [47], Video Captioning [55, 56], Image-text Retrieval [10, 41], and Visual Grounding [31, 41, 59]. The significance of language supervision has been demonstrated to provide valuable guidance for computer vision tasks [32, 42, 61]. In addition to one-hot vector labels, the semantic meaning and caption can also be taken into account, making traditional computer vision tasks more flexible and capable of handling open-world scenarios by identifying novel concepts in real-world applications and recognizing previously unseen categories.

To address the limitations of both MOT, which requires predefined categories and cannot handle unseen objects, and GMOT,

which relies on initial bounding boxes and struggles with various object features such as pose, illumination, scale, and texture, we propose a novel approach called zero-shot Generic MOT (Z-GMOT). Our proposed Z-GMOT draws inspiration from Grounded Language-Image Pretraining (GLIP) [31] and harnesses modern language models to enhance the flexibility and generality of MOT. However, we observe that GLIP generates many false positives when objects of the same category are presented in various attributes (e.g. color, shape). To minimize these false positives, we propose iGLIP, an improved version of GLIP.

Our proposed Z-GMOT framework follows the tracking-by-detection paradigm, which consists of two main stages: object detection and association. Our primary focus is on the detection stage, where we aim to detect unseen categories by leveraging the capabilities of a Vision-Language (VL) pre-trained model. The contributions of our work is four-fold: (i) we propose a novel Z-GMOT algorithm that can track never-seen object categories without any training examples, (ii) we eliminate the need for predefined categories as required in MOT and the initial bounding box as in GMOT, (iii) we introduce an improved version of GLIP, called iGLIP, which can detect unseen objects with low false positives, and (iv) we conduct extensive experiments, comparisons, and ablation studies on multiple datasets, including GMOT-40, AnimalTrack, and MOT17, to demonstrate the effectiveness and flexibility of the proposed Z-GMOT framework.

It is worth emphasizing that despite the simplicity of our proposed approach, its contributions are significant. Our study is expected to be of great interest to the MOT research community, as it demonstrates the potential of VL pre-trained models to pave the way for a new direction in tracking unseen object categories. We anticipate that our work will not only reduce the labeling effort required but will also inspire further research in the domain of unseen MOT and its potential extensions to other tracking scenarios.

## 2 RELATED WORK

### 2.1 Multiple Object Tracking - MOT

The state-of-the-art in MOT has been dominated by the tracking-by-detection paradigm, as demonstrated in various studies [2], [28], [52], [4], [7], and [63]. This approach typically involves detecting objects in each frame and then associating them over time. Recent MOT approaches can be broadly categorized into two types based on whether object detection and association are performed by a single model or separate models, known respectively as One-stage MOT and Two-stage MOT.

**One-stage MOT** *Joint detection and tracking* methods are classified as One-stage MOT, in which the detection and tracking steps are simultaneously produced in a single network. In this category, object detection can be modeled within a single network with re-ID feature extraction or motion features. YOLOTracker [9] is an end-to-end network for online detecting and tracking multiple objects. In CenterTrack [66], the authors used a simple method to train a network to predict the movement offset from the previous frame, and then matched it with the closest tracklet center point. QDTrack [40] is a combination of similarity learning and RCNN detection methods [20, 45], which randomly samples many region proposals within

a single pair of images. Trackformer [36] utilizes a novel tracking-by-attention mechanism and data association through the use of a Transformer network and querying new objects in an autoregressive context of tracklets. TraDeS [53] uses a joint online detection and tracking model that infers both object detection and segmentation. Unicorn [57] presents a unified model that addresses four different tracking problems with a single network, using the same input, backbone, head, and embedding for all tasks. MQT [26] proposed a transformer architecture with deformable attention for simultaneous tracking and appearance-based re-identification.

**Two-stage MOT Tracking-by-detection** is considered as a two-stage procedure: first, an object detection algorithm performs detecting objects in a frame, then those objects are associated with previous frame tracklets to assign identities for new objects. The SORT algorithm, as described in the paper by [2], presents a method for tracking multiple objects in real-time, online applications. Building on this, the authors of DeepSORT [52] added the use of appearance information to improve the performance of the tracking. This enhancement allowed for longer periods of occlusion to be handled. However, the OC-SORT [7] approach demonstrated that using a simpler motion model and focusing on observation during the recovery of lost tracks could achieve better results, even without the use of appearance information. ByteTrack [63] added a second-order association to associate all the detection boxes, including the low-confident ones, instead of only the high-scored boxes.

Our work Z-GMOT belongs to the second category, where we leverage VL pre-trained model to propose zero-shot object detector iGLIP and we flexibly associate with various tracking method.

## 2.2 Vision-Language

**Pre-trained models** Recent computer vision tasks are trained from VL supervision, which have shown strong transfer ability in improving model generality and open-set recognition. CLIP [42] is one of the first works effectively learning visual representations by large amounts of raw image-text pairs. After being released, it has received a tremendous amount of attention. Some other VL models ALIGN [24], ViLD [21], RegionCLIP [65], GLIP [31], UniCL[58], X-DETR [6], OWL-ViT [39], LSeg[30], DenseCLIP [43], OpenSeg [19], MaskCLIP [17] have also been proposed later to illustrate the great paradigm shift for various vision tasks. Based on case studies, we can categorize VL Pre-training models into (i) image classification e.g. CLIP, ALIGN, UniCL; (ii) object detection e.g. ViLD, RegionCLIP, GLIP, X-DETR, OWL-ViT and (iii) image segmentation e.g. LSeg, OpenSeg, DenseSeg. The first category is based on matching between images and language descriptions by bidirectional supervised contrastive learning (UniCL) or one-to-one mappings (CLIP, ALIGN). The second category contains two sub-tasks of localization and recognition. The third group involves pixel-level classification by adapting a pre-trained language-image model. In this work, we focus on object detection with GLIP.

**Visual Grounding** Visual grounding refers to the process of determining the precise correspondence between phrases in a sentence and objects or regions in an image. LSeg [30], OpenSeg [19], MaskCLIP [17], and DenseCLIP [43] directly adapt the pre-trained CLIP into pixel-level recognition tasks while handling class-agnostic mask generation. MDETR [25] is a network that detects

objects in an image based on a raw text query, such as a caption or question. The model uses a transformer-based architecture that allows for simultaneous reasoning over both text and image by integrating the two modalities early on in the model design. GLIP [31] combines the tasks of phrase grounding and one-stage object detection in that object detection can be considered as context-free phrase grounding, while phrase grounding can be seen as a context-dependent object detection task. TransVG [15] suggests using transformers to establish correspondence across multiple modes and demonstrates through evidence that using a stack of transformer encoder layers is simpler and more effective than using complex fusion modules. By distilling the knowledge from the CLIP/ALIGN model, ViLD [21] and RegionCLIP [65] are two-stage object detection methods, where a separate region proposal network (RPN) is used to distinguish foreground from background.

## 3 PROPOSED: ZERO-SHOT GMOT (Z-GMOT)

Our proposed Z-GMOT is a two-stage approach that follows the tracking-by-detection paradigm. The first stage involves object detection, where the success of VL pre-trained models is leveraged to propose an Improvement Grounded Language-Image Pretraining (iGLIP). The iGLIP model aims to detect never-seen object categories with fewer false positives than the original GLIP model [31], which is depicted in Figure 4(A). In the second stage, iGLIP is incorporated with various tracking methods for object association. The success of iGLIP in detecting never-seen object categories with zero training examples makes the proposed Z-GMOT algorithm highly flexible and effective in practical scenarios.

### 3.1 Zero-shot Object Detection: iGLIP

This section commences with a review of GLIP [31], followed by an in-depth analysis of its inadequacies in detecting object categories with distinct attributes. Subsequently, we propose iGLIP, an enhanced version of GLIP to mitigate false positives generated when objects presented with various properties. Finally, we explicate the association stage with various tracking methods.

#### i. GLIP - A Recap

GLIP [31] is a unified framework that reformulates object detection as phrase grounding. The general flowchart of GLIP is illustrated in Figure 4 (A). Specifically, GLIP extracts all word phrases from the input text prompt and passes them through a pre-trained language encoder (i.e., BERT [16]) to obtain  $M$  contextual word features  $P^0 \in \mathbb{R}^{M \times d}$ . Meanwhile, the input image is processed through an RPN-like network (i.e. DyHead [13]) to obtain a set of  $N$  proposals  $O^0 \in \mathbb{R}^{N \times d}$ . The deep fusion between visual embedding and text encoder is employed to match the textual phrases with the image proposals

#### ii. Limitations of GLIP

We empirically observe several limitations of GLIP as follows:

**Limitation 1: High False Positives.** GLIP demonstrates reliable performance for the general object category ( $OC^{Gen}$ ); however, it struggles to handle specific object categories ( $OC^{Spe}$ ) with property descriptions, such as color or shape. As shown in Figure 2, when various thresholds  $t$  are applied, the outcomes of GLIP's detection model for  $OC^{Gen}$  prompt (e.g., 'car') remain relatively stable. In



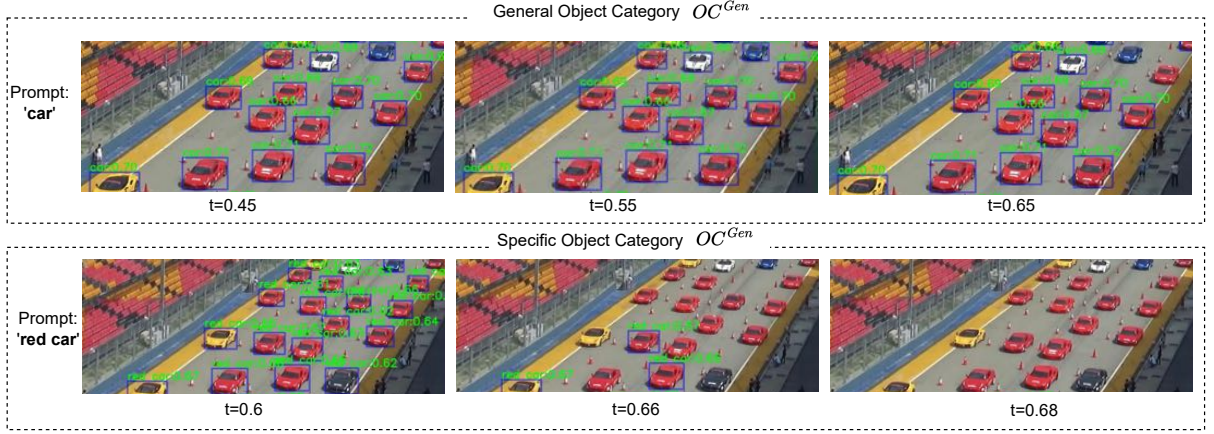


**Figure 2: Limitation 1 of GLIP [31].** Object detection by GLIP with different thresholds on two prompts: *car* (1<sup>st</sup> row) and *red car* (2<sup>nd</sup> row). While GLIP performs reliably on general object category  $OC^{Gen}$  *car*, it suffers from low TP (higher threshold) and high FP (lower threshold) when applied to specific object category  $OC^{Spe}$  *red car*.

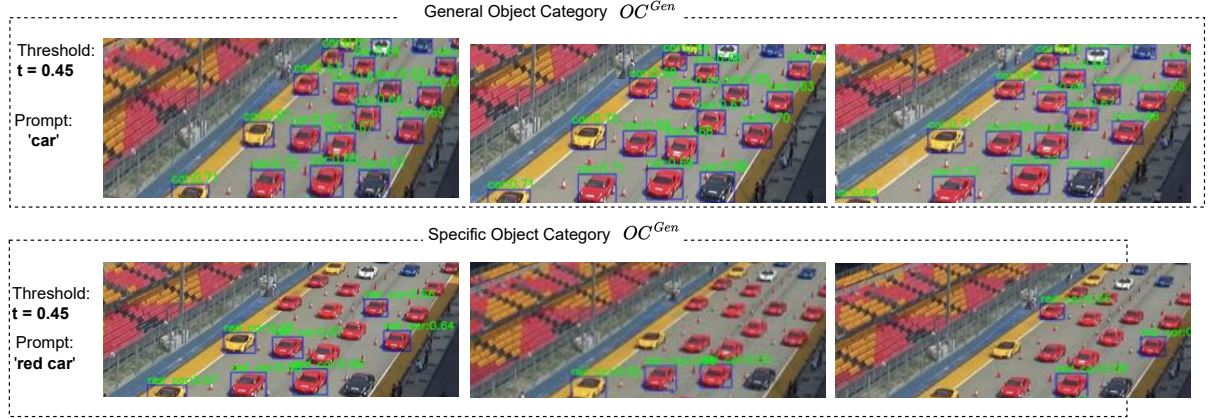


**Figure 3: Limitation 2 of GLIP.** Object detection by GLIP with the same threshold ( $t = 0.45$ ) on two prompts: *car* (1<sup>st</sup> row) and *red car* (2<sup>nd</sup> row) on different input images. While GLIP performs reliably for general object category  $OC^{Gen}$  *car*, it suffers from low TP and high FP when applied to specific object category  $OC^{Spe}$  *red car*.

contrast, for the  $OC^{Spe}$  prompt (e.g., 'red car'), the detected bounding boxes exhibit high variability, with true positives (TP) missing at high thresholds and false positives (FP) present at low thresholds. The trade-off between high TP and low FP makes it difficult to achieve optimal performance.

**Limitation 2: Deep fusion in GLIP weakens proposal features when dealing with specific object category.** The role of text embedding is critical in GLIP, as it has a significant impact on both token and proposal features. The token features  $P^i$  and proposal features  $O^i$  are fused through a deep fusion module, and thus the text embedding continues to influence proposal features throughout this module. In Fig. 3, we visualize the impact of the text embedding on GLIP's performance with the same threshold  $t$  for two cases of  $OC^{Gen}$  (i.e., 'car') and  $OC^{Spe}$  (i.e., 'red car'). While we obtain similar results on  $OC^{Gen}$ , the performance of GLIP is not reliable in the case of  $OC^{Spe}$ , even at the same threshold. Our empirical experiments suggest that the text embedding may either strengthen (in the case of  $OC^{Gen}$ ) or weaken (in the case of  $OC^{Spe}$ ) proposal features, despite the

presence of strong visual feature  $O^0$ . Our hypothesis is that GLIP focuses primarily on the object itself and does not pay adequate attention to its specific properties during the deep fusion process.

### iii. Our proposed iGLIP

In order to overcome the limitations of GLIP as discussed earlier, we propose iGLIP. To address *Limitation 1*, we propose a strategy where a **high threshold  $\mathcal{T}^h$**  is used for  $OC^{Spe}$  and a **low threshold  $\mathcal{T}^l$**  for  $OC^{Gen}$ . This way, only TP (no FP) are detected in  $OC^{Spe}$  while allowing for the acceptance of FP in the  $OC^{Gen}$ . The proposals from  $OC^{Spe}$  are treated as queries, and a **Query-Guided Matching** mechanism is proposed to filter all FP proposals from  $OC^{Gen}$ . Moreover, to address *Limitation 2*, we propose to utilize the rich visual features obtained from the backbone  $O^0$  instead of last layer feature  $O^0$  in our Query-Guided Matching. The overall architecture of our proposed iGLIP is illustrated in Fig. 4 (B).

iGLIP takes an input image  $I$  and two kinds of prompt, namely, the specific prompt ( $T_s$ ) and the general prompt ( $T_g$ ). Both kinds of prompts go through a text encoder, i.e., BERTModule [16] to obtain



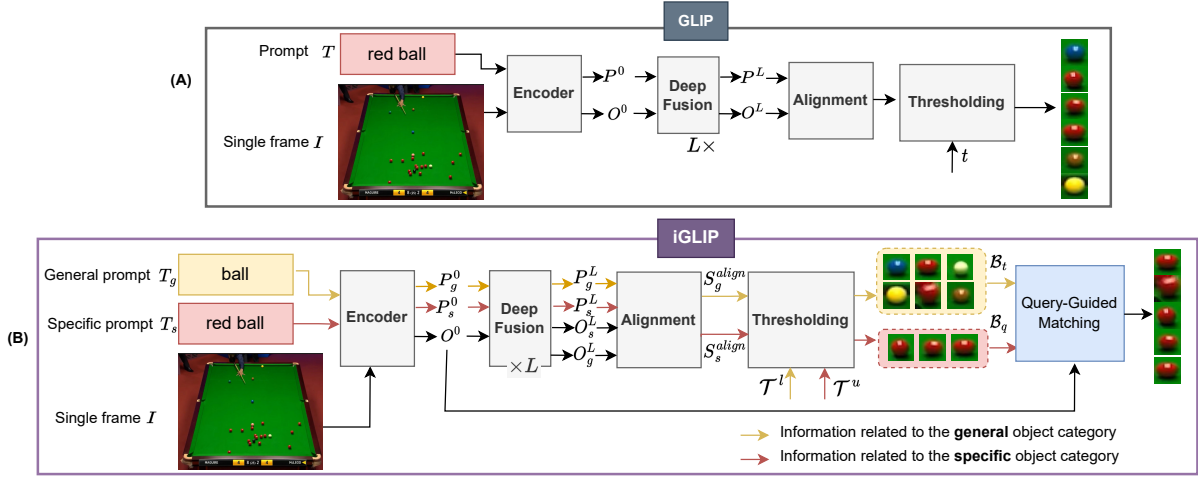


**Figure 4: Overall network architecture comparison between GLIP [31] (A) and our proposed iGLIP (B). Our iGLIP takes an image  $I$ , a general prompt  $T_g$ , and a specific prompt  $T_s$  as its input. iGLIP uses two thresholds  $\tau^u$  and  $\tau^l$ . iGLIP includes a Query-Guided Matching module to eliminate FP generated from the general prompt.**

contextual word features (i.e.,  $P_s^0$  and  $P_g^0$ ). Meanwhile, the input image goes through a visual encoder, i.e., DyHeadModule [13] to obtain proposal features (i.e.  $O^0$ ). Then,  $L$  deep fusion layers [31] are applied into  $P_s^0, P_g^0$  and  $O^0$  as follows:

$$O_s^0 = O^0 \text{ and } O_g^0 = O^0 \quad (1)$$

$$O_{s-t2i}^i, P_{s-i2t}^i = \text{X-MHA}(O_s^i, P_s^i), \quad i \in \{0, 1, \dots, L-1\} \quad (2)$$

$$O_{g-t2i}^i, P_{g-i2t}^i = \text{X-MHA}(O_g^i, P_g^i), \quad i \in \{0, 1, \dots, L-1\} \quad (3)$$

$$O_s^{i+1} = \text{DyHeadModule}(O_s^i + O_{s-t2i}^i), \quad O_s = O_s^L, \quad (4)$$

$$O_g^{i+1} = \text{DyHeadModule}(O_g^i + O_{g-t2i}^i), \quad O_g = O_g^L, \quad (5)$$

$$P_s^{i+1} = \text{BERTModule}(P_s^i + P_{s-i2t}^i), \quad P_s = P_s^L, \quad (6)$$

$$P_g^{i+1} = \text{BERTModule}(P_g^i + P_{g-i2t}^i), \quad P_g = P_g^L \quad (7)$$

Finally, the word-region alignment module is utilized to calculate the alignment score by performing a dot product between the deep fused features.

$$S_s^{\text{align}} = O_s P_s^\top, \text{ and } S_g^{\text{align}} = O_g P_g^\top \quad (8)$$

where  $O_s = O_s^L \in \mathbb{R}^{N \times d}$ ,  $O_g = O_g^L \in \mathbb{R}^{N \times d}$  are the visual features from the last visual encoder layer and  $P_s = P_s^L \in \mathbb{R}^{M \times d}$ ,  $P_g = P_g^L \in \mathbb{R}^{M \times d}$  are the word features of  $OC_{Spe}$  and  $OC_{Gen}$  from the last language encoder layer. The result of this operation are matrices  $S_s^{\text{align}} \in \mathbb{R}^{N \times M}$ ,  $S_g^{\text{align}} \in \mathbb{R}^{N \times M}$ . Each element  $S_s^{\text{align}}(i, j)$  represents the alignment score between the  $i$ -th proposal region and  $OC_{Spe}$ . Each element  $S_g^{\text{align}}(i, j)$  represents the alignment score between the  $i$ -th proposal region and  $OC_{Gen}$ .

The resulting bounding boxes are filtered by different thresholds, where a high threshold  $\tau^h$  is applied into  $S_s^{\text{align}}$  to ensure only TP are detected, and a low threshold  $\tau^l$  is applied into  $S_g^{\text{align}}$  to include all objects proposal, which may include FP. All the TP obtained by  $S_s^{\text{align}}$  are treated as a queries set  $B_q$  (i.e., template patterns), while all bounding boxes obtained by  $S_g^{\text{align}}$  form the target set  $B_t$ .

Query-Guided Matching module is then proposed to eliminate FP in  $B_t$  by using  $B_q$  as template patterns.

#### iv. Query-Guided Matching

To address the limitation of GLIP's deep fusion module not paying attention to specific properties, we propose a Query-Guided Matching mechanism to filter false positives from the general object category set  $B_c$ . Specifically, we use the TP obtained by the specific prompt as template patterns  $B_q$  and query back on  $B_c$  to find objects with similar visual properties. To perform the matching, we propose to utilize only visual features  $O^0$  extracted from the backbone (without the influence of text embeddings).

Let  $O_t^0$  and  $O_q^0$  represent the visual features of object proposals in  $B_t$  and  $B_q$ , the matching score is defined as the cosine similarity:

$$S_{qt} = \cos(O_q^0 \cdot O_t^{0T}), \quad (9)$$

The final detection results comprise the query objects and candidate objects with high similarity.

## 3.2 Target Association

After obtaining detection results from our zero-shot iGLIP model, we proceed to tackle the GMOT task by integrating it with a target association method. To evaluate the effectiveness of our proposed Z-GMOT, we conduct a comprehensive set of experiments on various association methods, including both conventional and more recent trackers with publicly available code, such as SORT [2], IOUTrack [3], DeepSORT [52], ByteTrack [63], OC-SORT [52].

A key distinguishing feature of our proposed approach, Z-GMOT, compared to existing methods in GMOT, is its ability to track object variants with a single inference. Current GMOT approaches rely on one-shot mechanisms and track objects in multiple inference, which can be limited in their ability to capture object variations. This difference is significant, as it simplifies the tracking process and increases efficiency by reducing the number of inferences required. By minimizing the need for repeated computations, Z-GMOT represents a promising advance in the field of MOT and GMOT that has

the potential to improve the speed and accuracy of object tracking in complex environments.

## 4 EXPERIMENT

### 4.1 Datasets & Metrics

For performance evaluation, we mainly benchmark our Z-GMOT on *GMOT-40* [1] and *AnimalTrack* [62] datasets.

**GMOT-40:** comprises 40 videos depicting 10 distinct categories of real-world objects, with each category consisting of 4 sequences. Each sequence contains objects belonging to the same category, commonly referred to as generic objects, and the average number of objects present in each frame is approximately 22. It is noteworthy that the GMOT-40 dataset does not contain any training data.

**AnimalTrack** consists of 58 video sequences of 10 common animal categories. Of these, 32 videos are designated for training, while the remaining 26 videos are designated for testing. In order to evaluate the efficacy of Z-GMOT, only the testing set is used.

To show the effectiveness of Z-GMOT on non-generic objects, complex objects, we further conduct ablation studies on the testing sets of *MOT17 dataset* [38] and *DanceTrack dataset*[50]. The MOT17 contains multiple instances of pedestrians, both indoor and outdoor. DanceTrack contains 100 videos of dancing people with 40 videos as trainset, 25 as valset and 35 as testset. We ignore all training data and conduct the experiment on MOT17-testset with 7 sequences and DanceTrack-testset with 35 videos.

We report and compare our performance on two kinds of metrics. **Standard MOT metrics:** High order tracking accuracy (HOTA), multiple object tracking accuracy (MOTA), mostly tracked targets (MT), mostly lost targets (ML), false positives (FP), false negatives (FN), ID switches (IDs). **ID metrics** [46] measure the correctness of the detection stage through the ratio of correct detections to the ground truth and predicted ones: identification precision (IDP), recall (IDR), and F1 score (IDF1).

### 4.2 Effectiveness of iGLIP

In this section, we evaluate the effectiveness of our proposed iGLIP by comparing it with the existing GLIP [31] in terms of detecting and tracking both general and specific object categories.

**Object detection:** We report the object detection comparison on the GMOT-40 dataset in Table 1. The first part of the table outlines the results for individual videos, while the second part presents the overall performance on the 40 videos of 10 categories within the GMOT-40 dataset. Our proposed iGLIP, which features a query-guided matching mechanism, can effectively handle both general and specific prompts, resulting in improved object detection performance compared to GLIP. Specifically, iGLIP achieves a significant improvement of 6.8 points in  $AP_{50}$  and 3.1 points in mAP, demonstrating its superiority over GLIP.

**Object Tracking:** Table 2 presents a comparison of the tracking of iGLIP and GLIP on two videos featuring specific objects, namely the ‘red ball’ in ‘ball-0’ video and ‘head light car’ in ‘car-1’ video. In addition, Table 3 illustrates the tracking performance comparison across the entire GMOT-40 dataset. It is evident that the improvements proposed in iGLIP result in enhanced performance for both specific and general object tracking.

**Table 1: Object detection comparison on G-MOT40 [1] between our iGLIP and GLIP [31]. The best score is in bold.**

Videos	Category		$AP_{50}$	$AP_{75}$	mAP
stock-3	‘wolf’	GLIP	73.6	57.2	48.7
		<b>iGLIP</b>	<b>78.7</b>	<b>59.2</b>	<b>51.1</b>
person-2	‘red athletic’	GLIP	30.8	24.1	21.5
		<b>iGLIP</b>	<b>45.4</b>	<b>42.0</b>	<b>35.4</b>
car-1	‘head light car’	GLIP	43.3	34.5	30.7
		<b>iGLIP</b>	<b>45.0</b>	<b>43.6</b>	<b>37.4</b>
ball-0	‘red ball’	GLIP	67.6	65.1	48.3
		<b>iGLIP</b>	<b>77.8</b>	<b>76.2</b>	<b>56.4</b>
40 videos	all 10 categories	GLIP	66.2	35.0	36.1
		<b>iGLIP</b>	<b>66.9 (+0.7)</b>	<b>40.0 (+5.0)</b>	<b>40.0 (+3.9)</b>

**Table 2: Tracking comparison between GLIP [31] and iGLIP in tracking specific objects i.e., ‘red ball’ in ‘ball-0’ video and ‘head light car’ in ‘car-1’ video with OC-SORT [7] association. The best score is in bold. Videos are from GMOT-40.**

	ball-0 video			car-1 video		
	HOTA	MOTA	IDF1	HOTA	MOTA	IDF1
GLIP [31]	69.56	51.98	80.34	41.92	29.76	54.98
<b>iGLIP</b>	<b>76.24</b>	<b>85.28</b>	<b>90.71</b>	<b>50.14</b>	<b>45.32</b>	<b>65.18</b>

**Table 3: Tracking comparison between GLIP [31] and iGLIP on GMOT-40 dataset. The best score is in bold.**

Tracker	Detector	HOTA↑	MOTA↑	FP↓	FN↓	IDF1↑
SORT	GLIP	53.08	51.61	53602	<b>60742</b>	60.01
	<b>iGLIP</b>	<b>54.21</b>	<b>62.90</b>	<b>12903</b>	74470	<b>64.34</b>
IOUTrack	GLIP	<b>47.59</b>	47.93	48054	<b>77134</b>	<b>49.39</b>
	<b>iGLIP</b>	46.08	<b>57.65</b>	<b>10517</b>	89075	48.27
DeepSORT	GLIP	49.31	44.84	71267	<b>59146</b>	53.95
	<b>iGLIP</b>	<b>50.45</b>	<b>58.99</b>	<b>25249</b>	69641	<b>57.55</b>
ByteTrack	GLIP	52.84	50.93	52787	<b>68984</b>	62.36
	<b>iGLIP</b>	<b>53.69</b>	<b>61.49</b>	<b>13609</b>	82157	<b>66.21</b>
OC-SORT	GLIP	55.20	52.51	47596	<b>71726</b>	63.33
	<b>iGLIP</b>	<b>56.51</b>	<b>62.76</b>	<b>10223</b>	83365	<b>67.40</b>



**Figure 5: An example where Z-GMOT receives low performance on FP and IDs. 1<sup>th</sup> row: Annotation in groundtruth. 2<sup>nd</sup> row: Bounding boxes detected by our iGLIP.**

### 4.3 Tracking Performance Comparison

This section presents a comparison of our proposed zero-shot-tracking Z-GMOT with other SOTA fully-supervised MOT methods

**Table 4: Performance comparison on GMOT-40 dataset [1] between our proposed Z-GMOT and other *one-shot-based GMOT methods* on various association methods. For each association method, the best scores are highlighted in bold.**

Tracker	Detector	Standard MOT metrics								ID metrics		
		HOTA↑	MOTA↑	FP↓	FN↓	IDs↓	MT↑	PT↑	ML↓	IDF1↑	IDP↑	IDR↑
MDP [54]	One-shot [1]	-	19.80	17260	186580	1779	142	621	1161	31.30	61.80	21.00
FAMNet [12]		-	18.00	20741	187730	1660	166	581	1197	28.30	54.80	19.10
MQT [27]		-	23.95	-	-	-	182	-	1077	31.06	-	-
SORT [2]	One-shot [1]	30.05	20.83	22337	176252	<b>5387</b>	241	<b>728</b>	975	33.90	59.37	23.72
<b>Z-GMOT/zero-shot</b>		<b>54.21</b>	<b>62.90</b>	<b>12903</b>	<b>74470</b>	8096	<b>1023</b>	671	<b>250</b>	<b>64.34</b>	<b>74.51</b>	<b>56.62</b>
IOUTrack [3]	One-shot [1]	24.53	15.17	11899	204006	<b>2827</b>	93	473	1378	26.22	<b>65.42</b>	16.39
<b>Z-GMOT/zero-shot</b>		<b>46.08</b>	<b>57.65</b>	<b>10517</b>	<b>89075</b>	11571	<b>768</b>	<b>727</b>	<b>449</b>	<b>48.27</b>	58.94	<b>40.88</b>
DeepSORT [52]	One-shot [1]	27.82	17.96	30982	173258	<b>9262</b>	252	<b>741</b>	951	30.37	49.31	21.94
<b>Z-GMOT/zero-shot</b>		<b>50.45</b>	<b>58.99</b>	<b>25249</b>	<b>69641</b>	12688	<b>1017</b>	698	<b>229</b>	<b>57.55</b>	<b>63.57</b>	<b>52.56</b>
ByteTrack [63]	One-shot [1]	29.89	20.30	21619	180714	<b>2571</b>	184	693	1067	34.70	63.09	23.93
<b>Z-GMOT/zero-shot</b>		<b>53.69</b>	<b>61.49</b>	<b>13609</b>	<b>82157</b>	3565	<b>810</b>	<b>805</b>	<b>329</b>	<b>66.21</b>	<b>78.29</b>	<b>57.35</b>
OC-SORT [7]	One-shot [1]	30.35	20.60	18545	183692	<b>2295</b>	181	610	1153	34.37	65.48	23.30
<b>Z-GMOT/zero-shot</b>		<b>56.51</b>	<b>62.76</b>	<b>10223</b>	<b>83365</b>	3245	<b>826</b>	<b>681</b>	<b>437</b>	<b>67.40</b>	<b>80.86</b>	<b>57.79</b>

**Table 5: Performance comparison on AnimalTrack testset [62] between our zero-shot Z-GMOT and existing *fully supervised MOT methods*. The best results on each metric are highlighted in bold.**

Tracker	Detector	Train	Standard MOT metrics								ID metrics		
			HOTA↑	MOTA↑	FP↓	FN↓	IDs↓	MT↑	PT↑	ML↓	IDF1↑	IDP↑	IDR↑
SORT [2]	Faster RCNN [45]	✓	42.80	55.60	<b>19099</b>	86257	<b>2530</b>	333	<b>470</b>	301	49.20	<b>58.50</b>	42.40
<b>Z-GMOT/zero-shot</b>		✗	<b>52.62</b>	<b>57.92</b>	49610	<b>42227</b>	6315	<b>599</b>	226	<b>91</b>	<b>57.96</b>	57.04	<b>58.90</b>
IOUTrack [3]	Faster RCNN [45]	✓	41.60	55.70	<b>25206</b>	77847	<b>4639</b>	388	<b>454</b>	262	45.70	<b>51.90</b>	40.70
<b>Z-GMOT/zero-shot</b>		✗	<b>47.79</b>	<b>59.93</b>	41482	<b>44500</b>	11418	<b>568</b>	257	<b>91</b>	<b>48.72</b>	49.04	<b>48.39</b>
DeepSORT [52]	Faster RCNN [45]	✓	32.80	41.40	<b>14131</b>	124747	<b>3503</b>	213	<b>452</b>	439	35.20	<b>49.70</b>	27.20
<b>Z-GMOT/zero-shot</b>		✗	<b>45.35</b>	<b>50.37</b>	67162	<b>40351</b>	14127	<b>591</b>	239	<b>86</b>	<b>48.09</b>	45.55	<b>50.94</b>
ByteTrack [63]	YOLOX [18]	✓	40.10	38.50	<b>31591</b>	116587	<b>1309</b>	310	<b>465</b>	329	51.20	<b>64.90</b>	42.30
<b>Z-GMOT/zero-shot</b>		✗	<b>51.31</b>	<b>58.58</b>	45903	<b>45172</b>	3157	<b>543</b>	276	<b>97</b>	<b>59.47</b>	59.38	<b>59.57</b>
OC-SORT [7]	YOLOX [18]	✓	<b>56.93</b>	<b>65.02</b>	<b>15881</b>	62253	<b>1561</b>	379	<b>402</b>	135	<b>67.48</b>	<b>76.17</b>	<b>60.58</b>
<b>Z-GMOT/zero-shot</b>		✗	55.06	63.16	39178	<b>42439</b>	2954	<b>571</b>	249	<b>96</b>	60.69	61.13	60.25

**Figure 6: Explore Z-GMOT in OV-MOT with various input queries on specific objects category. Left: OV-MOT on person with *red athletes*. right: OV-MOT on person with *green athletes*.****Figure 7: Explore Z-GMOT in OV-MOT with various input queries on specific objects category. left: OV-MOT on *wolf*. right: OV-MOT on *buffalo*.**

and one-shot-tracking GMOT on two datasets, namely the GMOT-40 and AnimalTrack datasets.

**Comparison with online/offline one-shot-GMOT methods:** One-shot-tracking GMOT, such as MDP [54], FAMNet [12], MQT [27],



**Table 6: Performance comparison on DanceTrack dataset between Z-GMOT and fully supervised MOT methods.**

Tracker	Detector	Train	HOTA	MOTA	IDF1
SORT [2]	YOLOX [18]	✓	47.80	88.20	48.30
<b>Z-GMOT/zero-shot</b>		✗	45.28	82.95	45.65
IOUTrack [3]	YOLOX [18]	✓	44.70	87.30	36.80
<b>Z-GMOT/zero-shot</b>		✗	38.57	82.06	32.29
DeepSORT [52]	YOLOX [18]	✓	45.80	87.10	46.80
<b>Z-GMOT/zero-shot</b>		✗	37.23	80.52	35.24
ByteTrack [63]	YOLOX [18]	✓	47.10	88.20	51.90
<b>Z-GMOT/zero-shot</b>		✗	42.98	81.47	46.84
OC-SORT [7]	YOLOX [18]	✓	52.10	87.30	51.60
<b>Z-GMOT/zero-shot</b>		✗	48.06	84.18	46.85

and GMOT [1], employ one-shot object detection [22] and use a tracking template in the first frame as input. These approaches do not require a training set, but their tracking performance depends heavily on the quality of the initial template, which may be affected by pose, resolution, illumination, and other factors. In contrast, our proposed Z-GMOT does not require a training set or an initial template.

To evaluate the performance of our Z-GMOT against existing one-shot-tracking methods, we compare it with online one-shot-tracking methods i.e., MDP [54], FAMNet [12], and MQT [27], and offline one-shot-tracking methods, GlobalTrack [22] integrated with SORT [2], IOUTrack [3], DeepSORT [52], ByteTrack [63], and OC-SORT [52]. For the offline methods, we follow the evaluation protocol in [33] and report the performance by running one-shot tracking GMOT five times, while for the online one-shot-tracking and our Z-GMOT, we report the results for a single inference.

Our Z-GMOT achieves remarkable improvements over both online and offline one-shot-tracking methods in terms of standard MOT metrics and ID metrics, despite not requiring any training samples. For example, using the same SORT association, our Z-GMOT surpasses 41.39 points MOTA and 35.18 points IDF1 the online one-shot-tracking MQT. Similarly, our Z-GMOT surpasses 25.47 points HOTA, 44.51 points MOTA, and 32.34 points IDF1 over offline one-shot-tracking methods with SORT association.

**Comparison with fully supervised MOT methods:** We evaluate our Z-GMOT on the AnimalTrack [62] dataset and compare its performance with other SOTA fully-supervised MOT methods. The AnimalTrack dataset contains multiple objects of the same animal category in each video, making it suitable for evaluating the GMOT task. Additionally, the dataset provides separate train/val/test sets, which can be used to train the fully supervised methods SORT [2], IOUTrack [3], DeepSORT [52], ByteTrack [63], and OC-SORT [52]. These methods train an object detector on the train set using either Faster RCNN [45] or YOLOX [18].

Our Z-GMOT, with zero training data, achieves comparable results to the fully-supervised methods on both standard MOT metrics and ID metrics. While the fully-supervised methods perform better in metrics such as FP, IDs, PT, and IDP, our Z-GMOT outperforms them in HOTA, MOTA, MT, ML, and IDF1, using the same tracker association. Notably, OC-SORT tracker and YOLO-X detector are considered to be the SOTA fully-supervised tracking method, and

our zero-shot Z-GMOT without training samples obtains very competitive performance.

#### 4.4 Ablation Study

In this section, we conduct ablation studies to evaluate the efficiency and effectiveness of our proposed Z-GMOT by examining various aspects as follows:

##### Investigate the failure cases by Z-GMOT

Table 4 and 5 exhibit impressive performance of Z-GMOT on GMOT and AnimalTrack datasets, surpassing other existing online/offline GMOT methods and compatible with fully-supervised MOT methods on unseen categories in the majority of metrics. However, as previously noted, Z-GMOT has limitations in terms of IDs and FP metrics. This section aims to investigate the cause of this issue further. As illustrated in Fig. 5, the absence of annotations for tiny objects such as ducks during evaluation leading high FP and IDs. Additional investigation will be included in the Supplementary.

##### Explore the potential of Z-GMOT in MOT track.

Table 6 presents the performance evaluation of Z-GMOT on the DanceTrack dataset [38] in comparison with other fully-supervised MOT methods. Despite not utilizing any training data, our proposed Z-GMOT achieves impressive results. For example, when using the SORT association, Z-GMOT achieves a HOTA of 45.28%, a MOTA of 82.95%, and an IDF1 of 45.65%, which is highly compatible with the performance of the fully-supervised MOT that employs YOLOX [18] as the object detector.

##### Explore the potential of Z-GMOT in Open-Vocabulary MOT (OV-MOT)

To illustrate a new problem of OV-MOT, we choose videos that contain several categories. Subsequently, we track individual objects category by different prompts to evaluate the adaptability of our proposed iGLIP and Z-GMOT to unseen categories and OV-MOT. As ground-truth data is not available for these categories, we report qualitative results in Figure 6 and Figure 7. Within the same video, our Z-GMOT allows to track different kinds of object ('red uniform' vs. 'green uniform', 'wolf' vs. 'buffalo'). This kind of work can open a new research direction in multiple generic MOT (MGOT). Our future investigation on OV-MOT will include conducting validation data for benchmarking.

## CONCLUSION & DISCUSSION

In this work, we have presented Z-GMOT, a zero-shot GMOT on unseen categories with zero training samples. Our Z-GMOT is a tracking-by-detection approach, where we have proposed iGLIP with query-guided matching mechanism to effectively detect unseen objects category. We evaluated the performance of iGLIP and Z-GMOT on various trackers, including SORT, IOUTrack, DeepSORT, ByteTrack, and OC-SORT. Our comprehensive experiments on GMOT-40, AnimalTrack, and DanceTrack datasets have demonstrated the superior performance of our Z-GMOT, which outperforms existing online/offline GMOT approaches and is highly compatible with fully-supervised MOT methods, even without any training samples is utilized in Z-GMOT. Our ablation studies further confirmed the advantage of iGLIP and Z-GMOT in recognizing and tracking objects with specific properties, with zero training data.

Our iGLIP and Z-GMOT introduce a novel method that utilizes the names of unseen categories to prompt a transductive zero-shot learning strategy, extending traditional MOT/GMOT to zero-shot MOT/GMOT and open vocabulary OV-MOT/GMOT tasks. Moreover, our work highlights the great potential of VL pre-trained models in tracking unseen categories, which can significantly minimize the labeling effort. We hope that our work will inspire future research in the unseen MOT/GMOT paradigm and its potential extensions to other tracking scenarios.

## REFERENCES

- [1] Hexin Bai, Wensheng Cheng, Peng Chu, Juehuan Liu, Kai Zhang, and Haibin Ling. 2021. GMOT-40: A benchmark for generic multiple object tracking. In *CVPR*. 6719–6728.
- [2] Alex Bewley, Zongyuan Ge, Lionel Ott, Fabio Ramos, and Ben Upcroft. 2016. Simple online and realtime tracking. In *ICIP*. IEEE, 3464–3468.
- [3] Erik Bochinski, Volker Eiselein, and Thomas Sikora. 2017. High-speed tracking-by-detection without using image information. In *AVSS*. IEEE, 1–6.
- [4] Guillem Brasó and Laura Leal-Taixé. 2020. Learning a neural solver for multiple object tracking. In *CVPR*. 6247–6257.
- [5] Holger Caesar, Varun Bankiti, Alex H Lang, Sourabh Vora, et al. 2020. nuscenes: A multimodal dataset for autonomous driving. In *Proceedings of the IEEE/CVF conference on computer vision and pattern recognition*. 11621–11631.
- [6] Zhaowei Cai, Gukyeon Kwon, Avinash Ravichandran, Erhan Bas, Zhuowen Tu, Rahul Bhotika, and Stefano Soatto. 2022. X-DETR: A Versatile Architecture for Instance-wise Vision-Language Tasks. *ECCV* (2022).
- [7] Jinkun Cao, Xinshuo Weng, Rawal Khrodgar, Jiangmiao Pang, and Kris Kitani. 2022. Observation-Centric SORT: Rethinking SORT for Robust Multi-Object Tracking. *arXiv preprint arXiv:2203.14360* (2022).
- [8] Nicolas Carion, Francisco Massa, Gabriel Synnaeve, Nicolas Usunier, Alexander Kirillov, and Sergey Zagoruyko. 2020. End-to-end object detection with transformers. In *ECCV*. Springer, 213–229.
- [9] Sixian Chan, Yangwei Jia, Xiaolong Zhou, Cong Bai, Shengyong Chen, and Xiaoqin Zhang. 2022. Online multiple object tracking using joint detection and embedding network. *Pattern Recognition* 130 (2022), 108793. <https://doi.org/10.1016/j.patcog.2022.108793>
- [10] Xinlei Chen, Hao Fang, Tsung-Yi Lin, Ramakrishna Vedantam, Saurabh Gupta, Piotr Dollár, and C Lawrence Zitnick. 2015. Microsoft coco captions: Data collection and evaluation server. *arXiv preprint arXiv:1504.00325* (2015).
- [11] Xin Wang Wenqi Xian Yingying Chen, Fangchen Liu Vashisht Madhavan Trevor Darrell, Fisher Yu, and Haofeng Chen. 2018. Bdd100k: A diverse driving dataset for heterogeneous multitask learning. *arXiv preprint arXiv: 1805.04687* (2018).
- [12] Peng Chu and Haibin Ling. 2019. Famnet: Joint learning of feature, affinity and multi-dimensional assignment for online multiple object tracking. In *Proceedings of the IEEE/CVF International Conference on Computer Vision*. 6172–6181.
- [13] Xiyang Dai, Yinpeng Chen, Bin Xiao, Dongdong Chen, Mengchen Liu, Lu Yuan, and Lei Zhang. 2021. Dynamic head: Unifying object detection heads with attentions. In *Proceedings of the IEEE/CVF conference on computer vision and pattern recognition*. 7373–7382.
- [14] Patrick Dendorfer, Hamid Rezaatofghi, Anton Milan, Javen Shi, Daniel Cremers, Ian Reid, Stefan Roth, Konrad Schindler, and Laura Leal-Taixé. 2020. Mot20: A benchmark for multi object tracking in crowded scenes. *arXiv preprint arXiv:2003.09003* (2020).
- [15] Jiajun Deng, Zhengyuan Yang, Tianlang Chen, Wengang Zhou, and Houqiang Li. 2021. Transvg: End-to-end visual grounding with transformers. In *ICCV*. 1769–1779.
- [16] Jacob Devlin, Ming-Wei Chang, Kenton Lee, and Kristina Toutanova. 2018. Bert: Pre-training of deep bidirectional transformers for language understanding. *arXiv preprint arXiv:1810.04805* (2018).
- [17] Zheng Ding, Jieke Wang, and Zhuowen Tu. 2022. Open-Vocabulary Panoptic Segmentation with MaskCLIP. *arXiv preprint arXiv:2208.08984* (2022).
- [18] Zheng Ge, Songtao Liu, Feng Wang, Zeming Li, and Jian Sun. 2021. YoloX: Exceeding yolo series in 2021. *arXiv preprint arXiv:2107.08430* (2021).
- [19] Golnaz Ghiasi, Xiuye Gu, Yin Cui, and Tsung-Yi Lin. 2022. Open-vocabulary image segmentation. *ECCV* (2022).
- [20] Ross Girshick. 2015. Fast r-cnn. In *ICCV*. 1440–1448.
- [21] Xiuye Gu, Tsung-Yi Lin, Weicheng Kuo, and Yin Cui. 2022. Open-vocabulary object detection via vision and language knowledge distillation. *ICLR* (2022).
- [22] Lianghua Huang, Xin Zhao, and Kaiqi Huang. 2020. Globaltrack: A simple and strong baseline for long-term tracking. In *AAAI*, Vol. 34. 11037–11044.
- [23] Drew A Hudson and Christopher D Manning. 2019. Gqa: A new dataset for real-world visual reasoning and compositional question answering. In *CVPR*. 6700–6709.
- [24] Chao Jia, Yinfei Yang, Ye Xia, Yi-Ting Chen, Zarana Parekh, Hieu Pham, Quoc Le, Yun-Hsuan Sung, Zhen Li, and Tom Duerig. 2021. Scaling up visual and vision-language representation learning with noisy text supervision. In *ICLR*. PMLR, 4904–4916.
- [25] Aishwarya Kamath, Mannat Singh, Yann LeCun, Gabriel Synnaeve, Ishan Misra, and Nicolas Carion. 2021. MDETR-modulated detection for end-to-end multimodal understanding. In *CVPR*. 1780–1790.
- [26] Bruno Korbar and Andrew Zisserman. 2022. End-to-end Tracking with a Multiquery Transformer. *arXiv preprint arXiv:2210.14601* (2022).
- [27] Bruno Korbar and Andrew Zisserman. 2022. End-to-end Tracking with a Multiquery Transformer. *arXiv preprint arXiv:2210.14601* (2022).
- [28] Laura Leal-Taixé, Cristian Canton-Ferrer, and Konrad Schindler. 2016. Learning by tracking: YOLO CNN for robust target association. In *CVPRW*. 33–40.

- [29] L. Leal-Taixé, A. Milan, I. Reid, S. Roth, and K. Schindler. 2015. MOTChallenge 2015: Towards a Benchmark for Multi-Target Tracking. *arXiv:1504.01942 [cs]* (April 2015). <http://arxiv.org/abs/1504.01942> arXiv: 1504.01942.
- [30] Boyi Li, Kilian Q Weinberger, Serge Belongie, Vladlen Koltun, and René Ranftl. 2022. Language-driven semantic segmentation. *ICLR* (2022).
- [31] Liunian Harold Li, Pengchuan Zhang, et al. 2022. Grounded language-image pre-training. In *CVPR*. 10965–10975.
- [32] Manling Li, Ruochen Xu, Shuohang Wang, Luowei Zhou, Xudong Lin, Chenguang Zhu, Michael Zeng, Heng Ji, and Shih-Fu Chang. 2022. Clip-event: Connecting text and images with event structures. In *CVPR*. 16420–16429.
- [33] Wenhao Luo and Tae-Kyun Kim. 2013. Generic Object Crowd Tracking by Multi-Task Learning. In *BMVC*, Vol. 1. 3.
- [34] Wenhao Luo, Tae-Kyun Kim, Bjorn Stenger, Xiaowei Zhao, and Roberto Cipolla. 2014. Bi-label propagation for generic multiple object tracking. In *CVPR*. 1290–1297.
- [35] Kenneth Marino, Mohammad Rastegari, Ali Farhadi, and Roozbeh Mottaghi. 2019. Ok-vqa: A visual question answering benchmark requiring external knowledge. In *CVPR*. 3195–3204.
- [36] Tim Meinhardt, Alexander Kirillov, Laura Leal-Taixé, and Christoph Feichtenhofer. 2022. Trackformer: Multi-object tracking with transformers. In *CVPR*. 8844–8854.
- [37] A. Milan, L. Leal-Taixé, I. Reid, S. Roth, and K. Schindler. 2016. MOT16: A Benchmark for Multi-Object Tracking. *arXiv:1603.00831 [cs]* (March 2016). <http://arxiv.org/abs/1603.00831> arXiv: 1603.00831.
- [38] Anton Milan, Laura Leal-Taixé, Ian Reid, Stefan Roth, and Konrad Schindler. 2016. MOT16: A benchmark for multi-object tracking. *arXiv preprint arXiv:1603.00831* (2016).
- [39] Matthias Minderer, Alexey Gritsenko, et al. 2022. Simple Open-Vocabulary Object Detection with Vision Transformers. *ECCV* (2022).
- [40] Jiangmiao Pang, Linlu Qiu, Xia Li, Haofeng Chen, Qi Li, Trevor Darrell, and Fisher Yu. 2021. Quasi-dense similarity learning for multiple object tracking. In *CVPR*. 164–173.
- [41] Bryan A Plummer, Liwei Wang, Chris M Cervantes, Juan C Caicedo, Julia Hockenmaier, and Svetlana Lazebnik. 2015. Flickr30k entities: Collecting region-to-phrase correspondences for richer image-to-sentence models. In *CVPR*. 2641–2649.
- [42] Alec Radford, Jong Wook Kim, Chris Hallacy, et al. 2021. Learning transferable visual models from natural language supervision. In *ICML*. PMLR, 8748–8763.
- [43] Yongming Rao, Wenliang Zhao, Guangyi Chen, Yansong Tang, Zheng Zhu, Guan Huang, Jie Zhou, and Jiwen Lu. 2022. Denseclip: Language-guided dense prediction with context-aware prompting. In *CVPR*. 18082–18091.
- [44] Joseph Redmon, Santosh Divvala, Ross Girshick, and Ali Farhadi. 2016. You only look once: Unified, real-time object detection. In *CVPR*. 779–788.
- [45] Shaoqing Ren, Kaiming He, Ross Girshick, and Jian Sun. 2015. Faster r-cnn: Towards real-time object detection with region proposal networks. In *NIPS*. 91–99.
- [46] Ergys Ristani, Francesco Solera, Roger Zou, Rita Cucchiara, and Carlo Tomasi. 2016. Performance measures and a data set for multi-target, multi-camera tracking. In *ECCV*. Springer, 17–35.
- [47] Oleg Sidorov, Ronghang Hu, Marcus Rohrbach, and Amanpreet Singh. 2020. Textcaps: a dataset for image captioning with reading comprehension. In *ECCV*. Springer, 742–758.
- [48] Amanpreet Singh, Vivek Natarajan, Meet Shah, Yu Jiang, Xinlei Chen, Dhruv Batra, Devi Parikh, and Marcus Rohrbach. 2019. Towards vqa models that can read. In *CVPR*. 8317–8326.
- [49] Alane Suhr, Stephanie Zhou, Ally Zhang, Iris Zhang, Huajun Bai, and Yoav Artzi. 2018. A corpus for reasoning about natural language grounded in photographs. *arXiv preprint arXiv:1811.00491* (2018).
- [50] Peize Sun, Jinkun Cao, Yi Jiang, Zehuan Yuan, Song Bai, Kris Kitani, and Ping Luo. 2022. Dancetrack: Multi-object tracking in uniform appearance and diverse motion. In *Proceedings of the IEEE/CVF Conference on Computer Vision and Pattern Recognition*. 20993–21002.
- [51] Longyin Wen, Dawei Du, Zhaowei Cai, Zhen Lei, Ming-Ching Chang, Honggang Qi, Jongwoo Lim, Ming-Hsuan Yang, and Siwei Lyu. 2020. UA-DETRAC: A new benchmark and protocol for multi-object detection and tracking. *CVIU* 193 (2020), 102907.
- [52] Nicolai Wojke, Alex Bewley, and Dietrich Paulus. 2017. Simple online and realtime tracking with a deep association metric. In *ICIP*. IEEE, 3645–3649.
- [53] Jialian Wu, Jiale Cao, Liangchen Song, Yu Wang, Ming Yang, and Junsong Yuan. 2021. Track to detect and segment: An online multi-object tracker. In *CVPR*. 12352–12361.
- [54] Yu Xiang, Alexandre Alahi, and Silvio Savarese. 2015. Learning to track: Online multi-object tracking by decision making. In *Proceedings of the IEEE international conference on computer vision*. 4705–4713.
- [55] Kashu Yamazaki, Sang Truong, Khoa Vo, Michael Kidd, Chase Rainwater, Khoa Luu, and Ngan Le. 2022. Vlcip: Vision-language with contrastive learning for coherent video paragraph captioning. In *2022 IEEE International Conference on Image Processing (ICIP)*. IEEE, 3656–3661.
- [56] Kashu Yamazaki, Khoa Vo, Sang Truong, Bhiksha Raj, and Ngan Le. 2022. VLTinT: Visual-Linguistic Transformer-in-Transformer for Coherent Video Paragraph Captioning. *arXiv preprint arXiv:2211.15103* (2022).
- [57] Bin Yan, Yi Jiang, Peize Sun, Dong Wang, Zehuan Yuan, Ping Luo, and Huchuan Lu. 2022. Towards Grand Unification of Object Tracking. In *ECCV*.
- [58] Jianwei Yang, Chunyuan Li, Pengchuan Zhang, Bin Xiao, Ce Liu, Lu Yuan, and Jianfeng Gao. 2022. Unified contrastive learning in image-text-label space. In *CVPR*. 19163–19173.
- [59] Licheng Yu, Patrick Poirson, Shan Yang, Alexander C Berg, and Tamara L Berg. 2016. Modeling context in referring expressions. In *ECCV*. Springer, 69–85.
- [60] Syed Sahil Abbas Zaidi, Mohammad Samar Ansari, Asra Aslam, Nadia Kanwal, Mamoon Asghar, and Brian Lee. 2022. A survey of modern deep learning based object detection models. *Digital Signal Processing* (2022), 103514.
- [61] Haotian Zhang, Pengchuan Zhang, et al. 2022. Glipv2: Unifying localization and vision-language understanding. *NIPS* (2022).
- [62] Libo Zhang, Junyuan Gao, Zhen Xiao, and Heng Fan. 2022. AnimalTrack: A Benchmark for Multi-Animal Tracking in the Wild. *IJCV* (2022), 1–18.
- [63] Yifu Zhang, Peize Sun, Yi Jiang, Dongdong Yu, Fucheng Weng, Zehuan Yuan, Ping Luo, Wenyu Liu, and Xinggang Wang. 2022. ByteTrack: Multi-Object Tracking by Associating Every Detection Box. In *ECCV*.
- [64] Zhong-Qiu Zhao, Peng Zheng, Shou-tao Xu, and Xindong Wu. 2019. Object detection with deep learning: A review. *IEEE TNNLS* 30, 11 (2019), 3212–3232.
- [65] Yiwu Zhong, Jianwei Yang, Pengchuan Zhang, et al. 2022. Regionclip: Region-based language-image pretraining. In *CVPR*. 16793–16803.
- [66] Xingyi Zhou, Vladlen Koltun, and Philipp Krähenbühl. 2020. Tracking Objects as Points. In *ECCV*. 474–490.



GMOT aims to track multiple objects of the same or similar generic type. However, current GMOT approaches such as [1, 33, 34] adopt the one-shot paradigm, which uses the bounding box of a single target object in the first video frame to track all objects that belong to the same class. The existing state-of-the-art (SOTA) GMOT is based on one-shot object detection. In this supplementary, we would like to discuss the following aspects:

- Discuss the strength and weaknesses of one-shot object detection.
- Discuss the strength and weaknesses of GLIP-based object detection.
- Report qualitative results for both detection and tracking tasks using our proposed iGLIP.

In our proposed iGLIP, specific objects are selected using a high threshold  $\mathcal{T}^u$ . We introduce two alternative solutions for defining the value of  $\mathcal{T}^u$ : a fixed value and a flexible value obtained from the top- $\kappa$  highest scores. In this supplementary, we provide ablation studies on the performance of iGLIP with respect to the two solutions for defining  $\mathcal{T}^u$  as follows:

- An ablation study on various high thresholds  $\mathcal{T}^u$ , whereas we fix the low threshold as 0.3, i.e.,  $\mathcal{T}^l = 0.3$ .
- An ablation study on various top- $\kappa$  highest confidence score.
- An ablation study of Z-GMOT on various backbones.
- Qualitative analysis of Z-GMOT.

All ablation studies in this supplementary have been conducted on GMOT-40 dataset [1] and SORT association [2].

In order to better illustrate our motivation and facilitate the analysis of the strengths and weaknesses of existing methods, we have classified objects into two groups: general objects, such as 'car', which may exhibit various attributes, and specific objects, such as 'red car', 'blue car', and 'yellow car', which possess particular attributes.

## A DISCUSSION OF ONE-SHOT OBJECT DETECTION.

The pros and cons of one-shot object detection is discussed as follows:

### Strength

In one-shot object detection, the initial bounding box serves as a template, which is subsequently matched with other object proposals, which are highly similar with the template. Thus, it enables effectively detect specific objects. This implies that a one-shot-based object detector can achieve high detection performance if all objects in a video exhibit highly similar properties, such as the same visual texture, resolution, illumination, and pose, as demonstrated in Fig. 8. Consequently, one-shot GMOT may perform well. However, such identical objects are rare in reality because objects of the same generic type such as insects, animal are living and moving, thus, they are presented in different poses, resolutions, occlusions, etc.

### Weakness

Although one-shot paradigm has been widely used in existing GMOT methods, it heavily relies on the initial bounding box and is limited in handling general objects, i.e., object variations, e.g., pose, illumination, occlusion, scale, texture, etc.

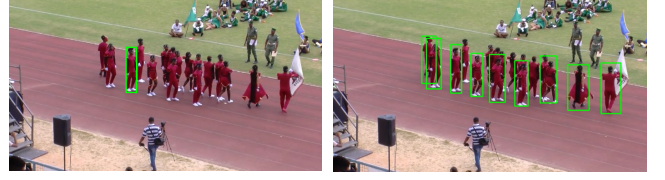


**Figure 8: An illustration of *strength* of one-shot object detector, which can detect specific objects, i.e. red athletic. Left: initial bounding box. Right: object detection by one-shot. The image is extracted from "person-2" video.**

Fig.9 (a) shows an example of different initial bounding boxes that result in different object detection and tracking. Fig.9 (b) illustrates an example where objects can not be detected and tracked if they are in different poses with the initial bounding box. Fig.9 (c) shows an example where objects are failed to be detected and tracked if they are in different resolutions with the initial bounding box. Particularly, this example highlights two scenarios where high-resolution objects are skipped if the target object is defined in low resolution or low-resolution objects are ignored if the target object is defined in high resolution. Fig.9 (d) depicts an example where objects can not be detected and tracked if they are in different textures.

As a result, one-shot object detection produces high False Negative (FN) on those objects of the same category with the template bounding box but represent in different attributes. Thus limiting its effectiveness in accurately detecting and tracking general objects.

## Strength and weakness of GLIP-based object detection

GLIP [31] is a unified framework that reformulates object detection as phrase grounding. A GLIP-based object detector utilizes input prompts to detect objects associated with them.

### Strength

GLIP demonstrates strong detection capabilities for general objects which is demonstrated in Figure 10. Compare to one-shot object detection in Fig.9, the GLIP-based object detector is more generalized and able to handle well general objects regardless of attributes.

### Weakness

Even GLIP-based object detector demonstrates a great potential in detecting general objects as shown in Fig.10; however, it suffers from a high rate of false positives. Furthermore, the GLIP-based object detector is limited deal with objects with specific characteristics/attributes as shown in Fig.11. For instance, when prompted to detect a 'red athletic', GLIP returns all person with various outfits and poses, which limits its ability to recognize objects with specific characteristics or attributes. In contrast, the one-shot object detection accurately detects specific objects as shown in Fig.8.

The aforementioned analysis shows that one-shot object detection is restricted in handling general objects whereas GLIP-based object detection struggles with detecting specific objects. In order to overcome these limitations, we propose iGLIP, which incorporates the strengths of both approaches. Specifically, iGLIP is designed to effectively detect both general and specific objects. We summarize the comparison between one-shot object detection, GLIP-based



Figure 9: Illustrations of *weakness* of one-shot object detection. For each example, the initial bounding box is on the left and one-shot object detection is on the right. (a): different initial bounding boxes resulting in different object detected, (b): objects of the same category at different poses with the initial template cannot be detected, (c): objects of the same category at different resolutions with the initial template cannot be detected, (d): objects of the same category at different texture with the initial template cannot be detected.

Table 7: Comparison between one-shot object detection, GLIP-based object detection, and our iGLIP object detection.

Object detection	General Object	Specific Object
One-shot	✗	✓
GLIP	✓	✗
iGLIP	✓	✓

object detection and our iGLIP as in the Table 7 in term of detection general object and specific object capability.

## B QUALITATIVE ANALYSIS OF THE PROPOSED IGLIP

In this section, we present a qualitative analysis of iGLIP on both general objects and specific objects. Being designed with both general prompt and specific prompt, iGLIP is capable of detecting various kinds of objects. The general prompt with low threshold  $\mathcal{T}^l$

is used to generate all possible proposals, but it can also result in a high rate of false positives. On the other hand, the specific prompt with high threshold  $\mathcal{T}^u$  is used to create high-confidence true positives that serve as queries. To address the issue of false positives in the general prompt and to find the best matches between specific objects and general object proposals, we propose a query-guided matching component in iGLIP. Fig.12 illustrates object detection by general prompt with  $\mathcal{T}^l$  (left), specific prompt with  $\mathcal{T}^u$  (middle) and iGLIP (right) with query-guided matching.

## C ABLATION STUDIES

### C.1 Ablation study on various threshold $\mathcal{T}^u$

Table 8 shows the tracking performance of iGLIP on the entire GMOT-40 dataset with seven different high thresholds  $\mathcal{T}^u$ . Furthermore, we also conduct an ablation study on particular videos from GMOT-40 dataset as shown in Table 9. In each video, we select various thresholds  $\mathcal{T}^u$ . In those experiments, we fix the lower



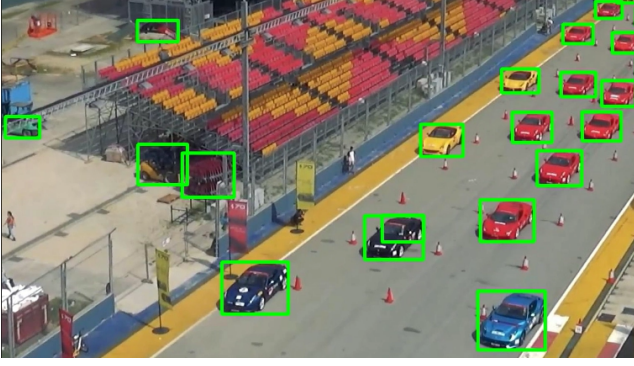


Figure 10: Illustrations of *strength* and *weakness* of GLIP in detecting general objects, i.e. ‘car’. While its strength lies in its ability to effectively detect all possible objects, GLIP still struggles with high false positives.



Figure 11: Illustration of *weakness* of GLIP in detecting specific objects, i.e., ‘red athletic’.

threshold  $\mathcal{T}^l$  to 0.3 ( $\mathcal{T}^l = 0.3$ ) to ensure that no true positives (TP) are missed and we use SORT association method. It is clear that with a smaller threshold  $\mathcal{T}^u$ , we obtain a high number of false positives (FP) and identity switches (IDs). This is because a smaller threshold allows for more bounding boxes to be selected from specific objects ( $OC^{Spec}$ ), resulting in high FP in the  $\mathcal{B}_q$  set. Since  $\mathcal{B}_q$  serves as the query, more FP in this set lead to more FP generated and more ID switches. Conversely, with a larger threshold  $\mathcal{T}^u$ , we obtain fewer FP and IDs. However, if the threshold is set too high, it may result in missing TP.

## C.2 Ablation study on various top- $\kappa$ highest score

With the second solution, we conduct the results on particular videos from GMOT-dataset. The performance of Z-GMOT on various threshold  $\mathcal{T}^u$  is shown in Table 10. Clearly, higher  $\kappa$  results in higher FP and may cause higher IDs. The solution of top- $\kappa$  provides similar performances compared to threshold  $\mathcal{T}^u$  selection; however, it seems to be more stable with smaller standard deviation. Thus, we use top- $\kappa$  selection in our Z-GMOT.

## C.3 Ablation study on various backbones

To show the effectiveness of our Z-GMOT on various backbones, we conduct an ablation study as shown in Table 11, where we compare the performance of Z-GMOT with two backbones i.e. Swin-T and Swin-L. In this ablation study, we choose one-shot GMOT, i.e., GlobalTrack with one-shot object detection [22] as a baseline. Even lower performance when Z-GMOT on Swin-L, Z-GMOT on Swin-T is still better than one-shot object GMOT [22] with resnet-50 is used.

## C.4 Ablation study on quantitative results of Z-GMOT

Fig.13 present quantitative results of Z-GMOT on three particular videos from GMOT-40 dataset. For each video, we randomly select three different frames. We also highlight some particular objects at each video to demonstrate the tracking capability.



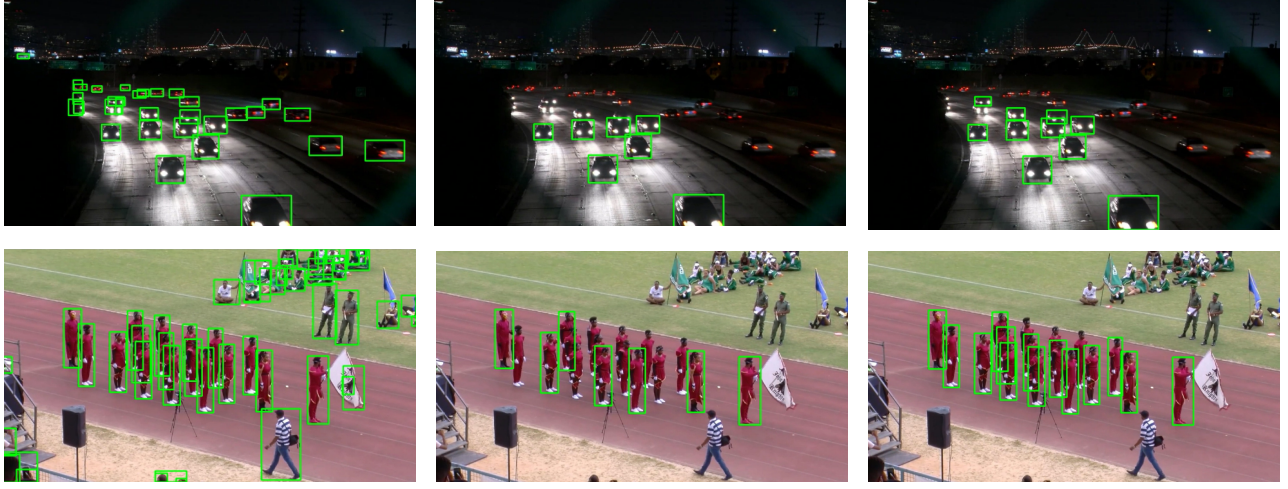


Figure 12: Qualitative performance of iGLIP in detecting both general objects and specific objects. From top to bottom: two videos from GMOT-40 dataset. From left to right: object detected by general prompt with  $\mathcal{T}^l$  (left), specific prompt with  $\mathcal{T}^u$  (middle) and iGLIP (right) with both  $\mathcal{T}^l$  and  $\mathcal{T}^u$  and query-guided matching.

Table 8: Ablation study with different high thresholds  $\mathcal{T}^u$  on GMOT-40 dataset.

$\mathcal{T}^u$	Standard MOT metrics								ID metrics		
	HOTA $\uparrow$	MOTA $\uparrow$	FP $\downarrow$	FN $\downarrow$	IDs $\downarrow$	MT $\uparrow$	PT $\uparrow$	ML $\downarrow$	IDF1 $\uparrow$	IDP $\uparrow$	IDR $\uparrow$
0.30	55.90	55.16	68736	37593	12041	1348	481	115	64.29	60.81	68.19
0.35	56.39	60.40	44742	49813	9378	1236	502	206	65.71	66.37	65.06
0.40	55.52	65.34	10057	72071	7120	969	719	256	66.24	76.81	58.23
0.45	49.65	49.58	20981	103285	6340	834	606	504	57.34	70.90	48.13
0.50	45.07	39.74	14415	136284	4780	615	597	732	50.10	72.81	38.19
0.55	41.14	32.21	9276	161961	3323	472	486	986	43.31	75.22	30.41

Table 9: Ablation study with different high thresholds  $\mathcal{T}^u$  on particular videos from GMOT-40 dataset.

Videos	General Prompt	Specific Prompt	$\mathcal{T}^u$	HOTA $\uparrow$	MOTA $\uparrow$	IDF1 $\uparrow$	FP $\downarrow$	FN $\downarrow$	IDs $\downarrow$
ball-0	ball	red ball	0.30	68.05	51.27	78.37	1862	43	64
			0.35	71.01	63.47	82.47	1376	45	60
			0.37	71.89	66.87	83.70	1239	49	59
			0.40	73.00	75.77	86.05	868	74	46
			0.43	71.98	74.82	85.51	758	227	42
			0.45	64.61	71.80	79.39	345	765	39
car-1	car	white car	0.53	57.65	31.62	68.74	2951	1596	119
			0.57	57.59	47.93	72.07	1323	2140	116
			0.60	45.37	44.61	62.94	195	3483	103
person-2	person	red uniform	0.35	42.77	19.04	44.19	4221	1609	151
			0.37	43.35	24.38	45.38	3823	1618	153
			0.45	51.38	60.93	60.33	580	2226	77
			0.50	50.99	62.95	58.88	373	2289	59
			0.53	51.35	61.53	59.14	285	2484	55

**Table 10: Ablation study with various top- $\kappa$  on three particular videos from GMOT-40 dataset.**

Videos	General Prompt	Specific Prompt	top- $\kappa$	HOTA	MOTA	IDF1	FP↓	FN↓	IDs↓
ball-0	ball	red ball	4	64.80	73.43	78.77	306	738	39
			5	67.24	75.04	81.48	372	610	39
			6	68.59	76.23	82.35	434	501	39
			7	70.48	76.68	84.42	518	399	36
			8	71.50	77.18	84.92	603	291	39
car-1	car	white car	4	57.30	56.39	74.23	438	2464	128
			5	59.24	54.67	74.87	871	2145	150
			6	59.62	50.14	73.93	1417	1899	138
			7	59.69	45.09	72.84	1958	1691	138
			8	59.26	39.56	71.43	2454	1565	140
person-2	person	red uniform	4	38.76	45.20	46.36	286	3655	67
			5	41.62	47.94	48.36	387	3352	84
			6	44.02	50.65	51.82	493	3054	89
			7	42.94	52.58	49.97	580	2820	99
			8	44.73	52.98	51.10	773	2598	113

**Table 11: Performance comparison between one-shot GMOT with backbone Resnet-50 and our proposed Z-GMOT with two different backbones (Swin-T and Swin-L) on GMOT-40 dataset. The best score is shown in bold.**

Tracker	Backbone	Detector	Standard MOT metrics								ID metrics		
			HOTA↑	MOTA↑	FP↓	FN↓	IDs↓	MT↑	PT↑	ML↓	IDF1↑	IDP↑	IDR↑
SORT	Resnet-50	One-shot	30.05	20.83	22337	176252	<b>5387</b>	241	<b>728</b>	975	33.90	59.37	23.72
	Swin-T	iGLIP	39.61	27.11	50517	131011	8831	587	692	665	44.12	54.22	37.19
	Swin-L	iGLIP	<b>55.52</b>	<b>65.34</b>	<b>10057</b>	<b>72071</b>	7120	<b>969</b>	719	<b>256</b>	<b>66.24</b>	<b>76.81</b>	<b>58.23</b>
IOUTrack	Resnet-50	One-shot	24.53	15.17	11899	204006	<b>2827</b>	93	473	1378	26.22	<b>65.42</b>	16.39
	Swin-T	iGLIP	33.05	23.53	46658	143436	11728	410	645	889	34.32	44.73	27.84
	Swin-L	iGLIP	<b>44.93</b>	<b>59.44</b>	<b>8655</b>	<b>86354</b>	11330	<b>697</b>	<b>794</b>	<b>453</b>	<b>46.87</b>	57.07	<b>39.77</b>
DeepSORT	Resnet-50	One-shot	27.82	17.96	30982	173258	<b>9262</b>	252	741	951	30.37	49.31	21.94
	Swin-T	iGLIP	36.71	21.92	65080	127577	14128	569	<b>742</b>	633	39.04	45.33	34.28
	Swin-L	iGLIP	<b>51.28</b>	<b>62.50</b>	<b>20178</b>	<b>66396</b>	11587	<b>995</b>	707	<b>242</b>	<b>58.30</b>	<b>64.71</b>	<b>53.04</b>
ByteTrack	Resnet-50	One-shot	29.89	20.30	21619	180714	<b>2571</b>	184	693	1067	34.70	63.09	23.93
	Swin-T	iGLIP	39.75	27.11	47795	136955	3968	462	726	756	45.93	58.18	37.94
	Swin-L	iGLIP	<b>55.29</b>	<b>64.09</b>	<b>10776</b>	<b>78836</b>	3289	<b>788</b>	<b>811</b>	<b>345</b>	<b>68.46</b>	<b>80.83</b>	<b>59.37</b>
OC-SORT	Resnet-50	One-shot	30.35	20.60	18545	183692	<b>2295</b>	181	610	1153	34.37	65.48	23.30
	Swin-T	iGLIP	41.34	29.12	41667	138463	3481	489	617	838	46.43	60.51	37.66
	Swin-L	iGLIP	<b>58.14</b>	<b>64.97</b>	<b>8916</b>	<b>79277</b>	2954	<b>787</b>	<b>700</b>	<b>457</b>	<b>69.76</b>	<b>82.96</b>	<b>60.19</b>



Figure 13: Qualitative tracking performance of Z-GMOT on particular videos. From top to bottom, video frames at different times. From left to right, we track ‘red ball’, ‘head light car’, ‘red athletic’.